Wang *et al. Herit Sci (2018) 6:4*
https://doi.org/10.1186/s40494-018-0168-3

Heritage Science

RESEARCH ARTICLE

The method to soften the concretions of ceramics in the "Nanhai I" Shipwreck of China Southern Song Dynasty (1127–1279AD)

Yanrong Wang[1], Tiequan Zhu[1*], Guicheng Yang[2], Xian Tan[3], Daoyang Ye[3] and Haotian Chen[3]

Abstract

The "Nanhai I" shipwreck of the Southern Song dynasty is the existent oldest and the most integrally preserved shipwreck in the world. Inside the shipwreck most of the ancient ceramics were covered with different types of concretions. In our work, different types of concretions were analyzed using stereomicroscopy, X-ray fluorescence (XRF) and X-ray diffraction (XRD). Based on those analyses, we applied a new physical method of heating and boiling to soften the concretions and remove them from the ceramics. It turned out that this method was efficient to remove the white shellfish concretions, gray concretions and red iron concretions, which not only provided a good basis for the preservation of ancient ceramics of the shipwreck, but also benefited the archaeological research on ancient ceramics.

Keywords: "Nanhai I" shipwreck, Ceramics, Concretions, Heating and boiling

Introduction

Located around 20 nautical miles south of Dongping port in Yangjiang city, the "Nanhai I" shipwreck was found as shown in Fig. 1. Based on the excavation reports, the "Nanhai I" shipwreck is dated to the Southern Song dynasty of China (1127–1279AD). It was firstly discovered in 1987, then salvaged and integrally raised from the sea in 2007. According to the preliminary calculations, this shipwreck has more than 6000 items on board and most of them are ceramics [1]. These ceramics are good materials to study the history of ancient ceramics, as well as their maritime trades. Although lots of ceramics from shipwrecks still have beautiful outward appearance without concretions [2, 3], due to the impact of seawater and other harmful factors, another part of ceramics more or less have corroded or covered the concretions. For "Nanhai I" shipwreck, a number of ceramics have been greatly corroded and covered with different types of concretions including seabed sediments, shellfishes and other substances. The concretions not only conceal the elegant and fine appearance of these ceramics, but also hamper further analyses on the ceramics themselves, and their conservation. Therefore, removing the concretions and restoring the ceramics to their pristine appearance is one of the conservators' main tasks.

In the early 1970s, many researchers were already devoted to the preservation of ancient shipwrecks and their cargo [4–8]. In 1980s, with the discoveries and excavations of numerous ancient shipwrecks in China, more and more Chinese scientists started to work on the preservation of ancient artifacts from shipwrecks. Yang Heng and Tian Xingling in Institute of Cultural Relic Research and Archaeology of China applied XRF, XRD and SEM–EDS to analyze the corrosion of brown artifacts in the "Nan'ao I" shipwreck and found that the corrosion products mainly contained $CaCO_3$, $CaSiO_3$ and Ca_2SiO_4. Based on the analyses, mechanical tools were chosen to remove the concretions [9, 10]. In 2013, Liu Wei and Zhang Zhiguo analyzed concretions of iron wares from three shipwrecks including "Nanhai I", "Nan'ao I" and "Huaguangjiao I" with using multiple scientific techniques. They found that concretions from the "Huaguangjiao I" and "Nan'ao I" mainly contained iron (Fe_3O_4,

*Correspondence: zhutq@mail.sysu.edu.cn
[1] School of Sociology and Anthropology of Sun Yat-sen University, No.135, Xingangxi Rd, Guangzhou 510275, China
Full list of author information is available at the end of the article

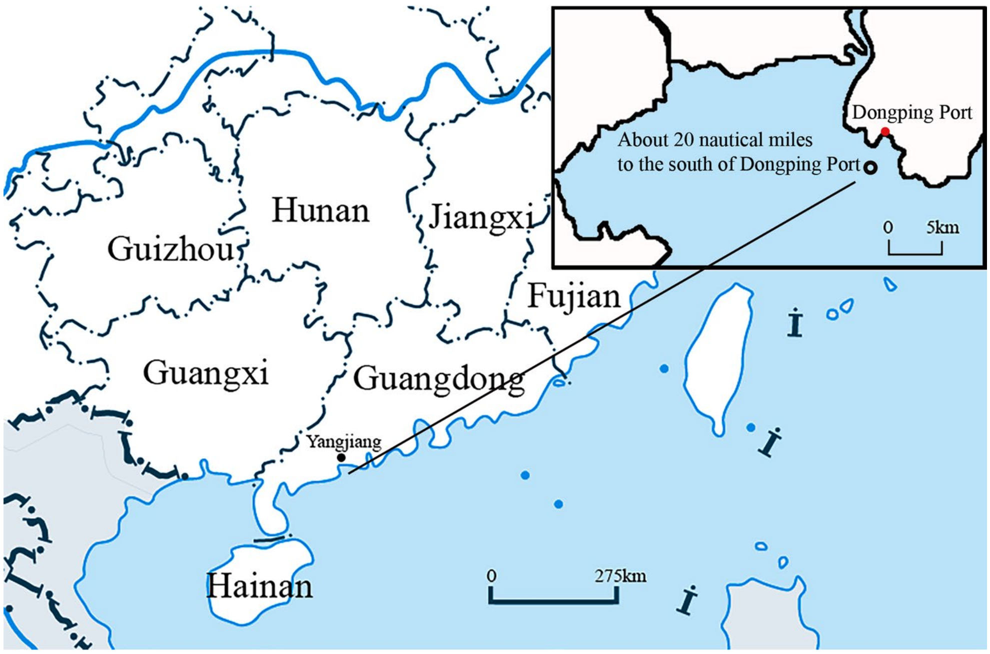

Fig. 1 Geological location of "Nanhai I" shipwreck

α-FeOOH, γ-FeOOH, Fe2O3 and some $Fe_8(OOH)_{16}Cl_{1.3}$), and calcareous concretions (aragonite and calcite), while concretions from the "Nanhai I" shipwreck contained calcareous and siliceous concretions. After that, the forming mechanism of concretions was discussed [11]. Moreover, some scholars also applied chemical methods to remove the concretions. For instance, Ma Yanru in the National Museum of China detected the chemical composition of the concretions from the "Huaguangjiao" shipwreck. Based on her analyses, chemical resolution was chosen to remove the concretions. A combination of 3% citric acid and 5% EDTA-2Na was adopted to soften the concretions [12, 13]. In addition, Bao Chunlei of Hainan Provincial Museum also analyzed different types of iron concretions from the "Huaguangjiao I" shipwreck and chose EDTA-2Na (in order to dissolve calcareous concretions without harming the iron products) with 10% sodium thioglycolate or 5% oxalic acid (to dissolve the brown rust) to remove the concretions [14].

The researches mentioned above are of great importance for the removal of concretions in the "Nanhai I" shipwreck. However, considering lots of glazed ceramics in the shipwreck which would be easily eroded by acid, the chemical method doesn't seem to be a suitable method in this case. In our work, different types of concretions were analyzed, using X-ray fluorescence spectrometry (XRF) and X-ray diffraction (XRD). Based on those analyses, a physical method consisting of heating and boiling to soften and remove the concretions from ceramics in the "Nanhai I" shipwreck was tested.

Experimental details

Sample description

Twenty-seven samples with different concretions from the "Nanhai I" Shipwreck (provided by Maritime Silk Road Museum of Guangdong, China) were selected for the experiment. All samples were dated to the Southern Song dynasty (1127–1279AD). From the appearance of the concretions, the samples were divided into four categories: white shellfish concretions, gray concretions, brown concretions and shallow gray concretions. Typical samples are shown in Fig. 2: Sample N09 (Fig. 21(a)) is one of white shellfish samples. Its concretion, only one small piece of white shell adheres inside the ceramic fragment. Sample N20 (Fig. 22(a)) is one of gray concretions. The gray concretion covers almost half of white ceramic fragment. Inside the concretion, there also have smaller ceramic fragments. Sample N14 (Fig. 23(a)) and N25 (Fig. 24(a)) are brown concretions. The ceramic pieces here are very small and completely covered in the concretions. Sample N21 is shallow gray concretions (Fig. 25).

Microscopy observations

The concretion samples were observed with the Stereomicroscope (SMZ1500 Nikon, Japan), and the software used for image collection and analyses was the NIS-Elements D4.10.00.

Fig. 2 The photograph of the samples from the "Nanhai I" Shipwreck: **1a** Sample N09 with concretion before the treatment. **1b** Ceramic fragment of Sample N09 without concretion after the treatment; **2a** sample N20 with concretion before the treatment; **2b** Ceramic fragments of Sample N20 without concretion after the treatment; **3a** Sample N14 with concretion before the treatment. **3b** Ceramic fragments of Sample N14 without concretion after the treatment; **4a** sample N25 with concretion before the treatment; **4b** Ceramic fragments of Sample N25 without concretion after the treatment; **5** sample N21 with concretion

Micro X-ray spectroscopy analyses

Micro X-ray Spectroscopy (EAGLE-III.XXL, USA) was employed to analyze the chemical composition of the samples. It was operated in the voltage of 40 kV and current of 200 mA of the X-ray tube, vacuum optical route and a beam spot size of 300 μm. The resolution was 137.5 eV at Mn–Ka and the dead time was close to 30%. The software for spectrum collection and analysis was the VISION32 program connected with the instrument.

X-ray diffractometer investigation

MXP18AHF X-ray diffractometer (Mc. Japan) was equipped with a Cu X-ray tube, and operated at 40 kV and 100 mA. And DS, SS and RS were respectively 1, 1 and 0.15 mm. It was used to analyze the crystalline structure of the samples.

Physical heating exploration

Based on XRF and XRD results, a physical heating protocol was adopted (Fig. 3):

1. Put the samples in the blast drying chamber for 1.5 h at the temperature of 170 °C;
2. If the concretions become soft and loose, remove them using a scalpel pry; if not, put them into the water bath at the temperature of 100 °C for 3 h. If then the concretions become soft and loose, remove the concretions using a scalpel pry; if not, repeat the heating process.

The heating blast drying chamber (DHG—9140, Shanghai Three Scientific Instruments Ltd.) was used to heat the samples, and an electro-thermostatic water bath (HWS26, Shanghai Yiheng Scientific Instrument Co., Ltd.) was applied to boil the samples.

The main purpose of using a physical method was to avoid acid corrosion on the ceramics glaze and to eliminate the concretions without damaging the ceramics.

Compressive strength tests

In material science, the Peierls Stress is the maximum force that a material can bear before cracking, which is often used to describe the fragility and vulnerability of the material.

The tests were carried out in Sun Yat-sen University, using Electro-mechanical universal testing machine (WD-5A, Guangzhou Laboratory Instrument Company Limited). Because of its destructive characteristic, different modern materials including pottery and porcelain were used instead in this test. The sample preparation is as follows:

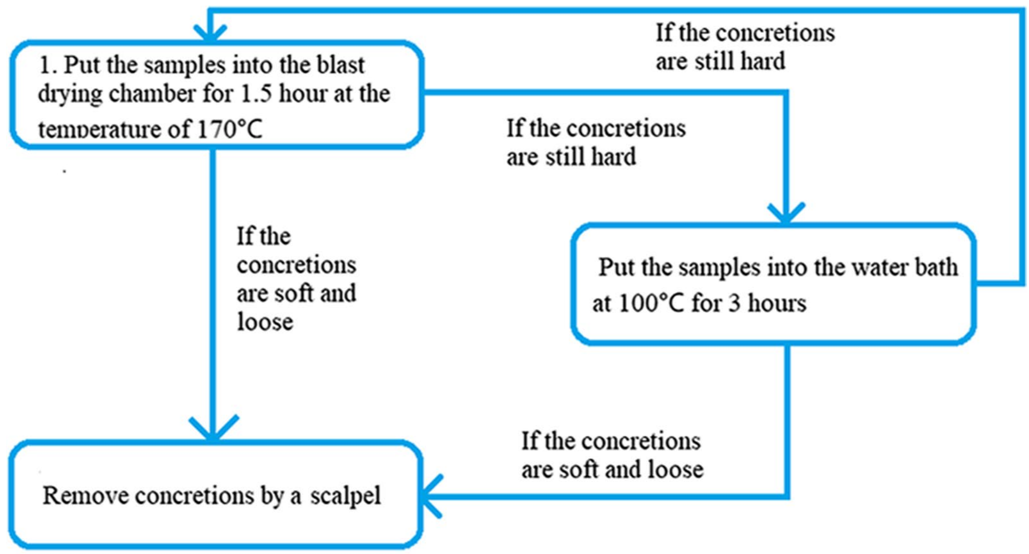

Fig. 3 Process of the treatment

- Cut pottery and porcelain into square samples with the length of 10 mm (permissible variations might be 10 ± 3 mm);
- place square samples on test stage;
- apply different pressures from 0 N to the pressure that would cause the cracking of the sample.

The experiment operations followed the national standard of China [15].

Results

Microscopy observations on the samples

The microscopy analyses were mainly carried out on the surface of the concretions but also in the interface between the concretions and the glaze of all the samples. The surface, the interface and the pores between the particles were observed under the microscope (Fig. 4a). Besides, some crevices between the concretions and the glaze were also spotted (Fig. 4b), which implies the softness and porous texture of some gray samples. Reddish and brown particles (Fig. 4c, d) between the concretions and the glaze were also observed, as well as the excreta or secretions of marine shellfish (Fig. 4e). And the shadow gray concretions (Fig. 4f) had a more complex nature. They are composed of quartz with size of 0 ~ 1 mm, shell debris with size of 2–3 mm and smaller white particles. The shadow gray concretions contained tight and dense particles concreted together, and meanwhile there were some holes between the shells and quartz on the surface.

Micro X-ray spectroscopy analyses

The results of quantitative XRF analyses before physical heating are given in Table 1. The measurements were carried out on the surface of most samples in the red, gray and white areas except shellfish samples. In each colored areas, three points were analyzed and an average was calculated. The analyses show that, the amount of silicon, calcium and iron changes quite obviously, respectively ranging from 1.19 to 86.67%, 0.33 to 81.76% and 0.95 to 69.52%. And most individual samples contain these three elements, but the content varies, depending on the type of concretion. For instance, the amount of silicon in the gray region is as high as 49.53–86.67%, calcium in the shadow-white area is 34.06–81.76%. The percentage of iron (9.71–69.52%) and sulfur (1.62–24.82%) is also very high in the brown area. Thus, gray concretions mainly contain silicon (Si) and calcium (Ca), while brown concretions with red, dark red and brown particles contain silicon (Si), calcium (Ca), iron (Fe) and sulfur (S).

In order to better understand the chemical changes before and after the heating and boiling process, two typical samples (sample N23 and N25) were re-analyzed after the treatments. The comparative results regarding the composition are shown in Table 2. After physical heating and boiling, the amount of sulfur decreased, while the amount of iron increased.

X-ray diffraction results

XRD was used to determine the crystalline composition in gray and red particles. The measurements were carried

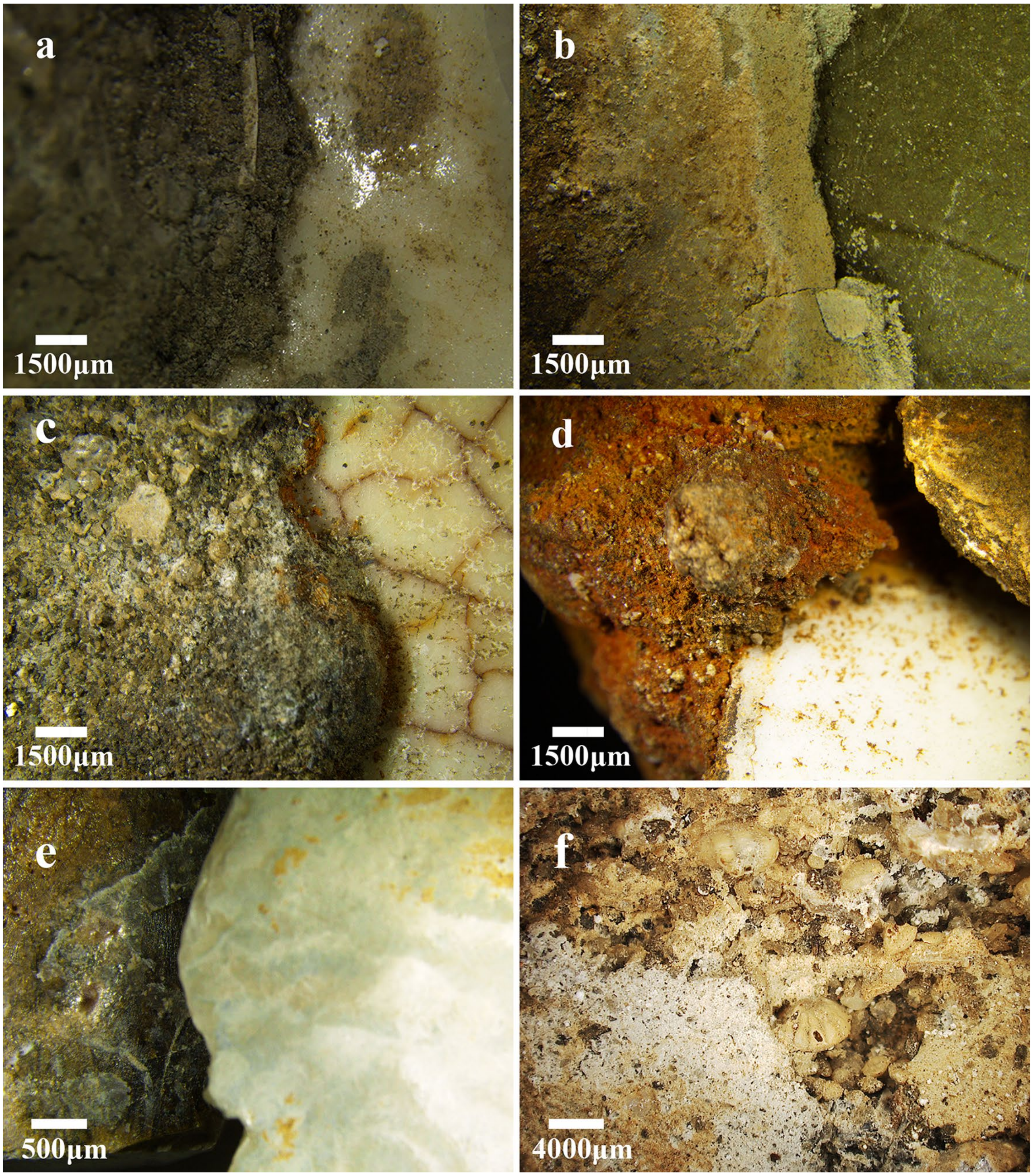

Fig. 4 Micrograph on typical samples: **a** The interface of sample N20; **b** the interface of sample N22; **c** the interface of sample N3; **d** the interface of sample N23; **e** the interface of sample N7; **f** the surface of N21

out on typical samples: gray concretions on the N26, N21 samples and brown concretions on the N23 and N25 samples. In particular, brown concretions from the N23 and N25 samples were re-assessed using XRD investigation after physical heating process.

Figure 5a shows the X-ray diffraction spectrum of the N26 gray powder. The peaks at 4.26, 3.34, 2.46, 1.81 and 1.54 Å are consistent with α-quartz, while 3.85, 3.04, 2.28, 1.98 and 1.88 Å are consistent with calcite. It suggests that the main phases of the N26 gray powder are quartz and calcite, and those of another sample the N21 (Fig. 5b) are α-quartz, aragonite, calcite and feldspar.

In Fig. 5c and d, the XRD spectrums of brown concretions reveal the existence of pyrite, gypsum and α-quartz. The characteristic diffraction peaks of pyrite (FeS_2) decrease in these two samples after heating and

Table 1 The analytical results of the concretions of different samples by μ-XRF (wt %)

Samples	wt%											
	Na_2O	MgO	Al_2O_3	SiO_2	SO_3	K_2O	CaO	TiO_2	Cr_2O_3	MnO	Fe_2O_3	CuO
N1-1grey	1.86	9.14	12.18	62.48	1.74	1.29	6.53	0.73	0.09	0.13	3.71	0.03
N1-1white	1.78	5.76	3.59	10.77	0.39	0.57	75.53	0.15	0.06	0.11	0.95	0.06
N2-1white	1.28	3.14	1.03	1.19	1.20	0.43	89.10	0.03	0.08	0.17	1.26	0.08
N2-1red	1.60	13.83	6.43	30.81	7.46	0.26	3.92	0.19	0.11	0.34	34.76	0.15
N3-1white	2.65	4.94	1.35	4.95	2.38	0.42	81.75	0.01	0.05	0.02	1.12	0.01
N3-1red	3.61	2.07	7.04	32.50	6.45	1.52	2.16	0.23	0.15	0.31	43.82	0.04
N4-1white	0.82	7.77	1.49	4.40	1.85	0.64	72.78	1.00	0.04	0.17	7.64	0.03
N5-1grey	2.31	3.12	7.41	68.26	4.39	0.83	7.99	0.53	0.08	0.19	4.51	0.12
N5-1white	1.42	6.58	2.28	14.06	3.12	0.51	68.12	0.06	0.06	0.29	3.05	0.05
N5-1red	1.77	5.34	3.82	11.20	4.61	0.39	21.30	0.23	0.12	0.39	50.18	0.02
N6-1red	1.67	0.65	5.26	18.65	1.62	0.52	0.94	0.24	0.11	0.72	69.51	0.02
N8-1white	0.54	1.69	1.88	10.60	7.61	0.52	56.84	0.25	0.12	0.22	19.21	0.03
N8-1red	4.20	2.29	4.82	19.22	24.82	0.48	7.90	0.20	0.19	0.28	35.47	0.04
N10-1red	2.27	1.98	4.53	31.18	5.37	0.80	1.58	0.33	0.14	0.22	51.18	0.04
N11-1red	9.50	8.67	7.90	6.99	19.73	0.04	0.33	0.09	0.13	0.28	46.27	0.01
N12-1white	1.11	13.33	4.61	29.29	5.08	0.81	40.81	0.22	0.04	0.11	4.37	0.01
N12-1red	1.85	5.24	1.59	20.42	19.58	0.45	22.17	0.14	0.12	0.30	27.88	0.03
N13-1red	1.46	1.40	14.72	40.64	2.28	2.57	0.58	1.00	0.06	0.11	34.96	0.05
N14-1grey	1.13	9.10	3.50	65.20	1.99	1.11	15.32	0.19	0.08	0.08	1.93	0.04
N14-1white	2.97	10.16	3.52	11.69	0.69	1.58	57.69	0.71	0.08	0.56	9.71	0.03
N14-1red	2.05	20.04	10.14	49.94	1.66	1.95	0.99	0.53	0.03	1.32	11.22	0.03
N15-1white	3.95	6.01	5.19	22.35	2.45	0.98	51.12	0.32	0.08	0.23	5.92	0.07
N15-1red	3.83	1.83	2.97	10.42	5.81	0.11	5.32	0.17	0.12	0.38	68.77	0.08
N16-1grey	1.33	1.82	2.9	72.65	9.78	0.60	7.11	0.26	0.03	0.08	3.20	0.12
N16-1white	1.34	5.40	5.75	22.32	2.59	1.23	51.31	2.16	0.08	0.16	7.25	0.08
N16-1red	2.49	6.27	10.65	44.57	7.75	1.78	8.99	0.60	0.06	0.24	16.41	0.06
N17-1white	2.33	3.14	10.72	57.50	7.62	3.07	7.21	0.20	0.04	0.21	7.69	0.03
N17-1red	2.50	1.75	7.07	27.03	10.64	1.45	1.07	0.26	0.13	0.24	47.39	0.05
N18-1white	1.72	3.94	3.37	9.55	2.53	1.03	67.69	0.32	0.04	0.30	7.67	0.04
N19-1grey	2.82	6.84	5.53	60.80	2.25	1.21	16.58	0.09	0.04	0.10	3.54	0.03
N19-1white	0.42	6.79	6.22	24.61	3.57	3.11	46.35	0.44	0.05	0.18	7.76	0.09
N20-1grey	1.17	9.20	13.97	61.45	1.82	3.49	4.07	0.57	0.02	0.22	3.88	0.02
N20-1white	1.51	8.56	1.67	4.54	0.46	0.59	77.70	0.33	0.03	0.65	3.63	0.02
N21-1grey	1.82	1.58	2.54	86.67	1.41	0.16	4.86	0.05	0.02	0.19	0.46	0.01
N21-1white	0.69	3.03	4.52	10.02	0.72	1.43	73.32	0.41	0.07	0.24	3.91	0.12
N22-1grey	1.58	7.32	11.56	51.38	6.14	1.87	13.44	0.63	0.07	0.18	5.6	0.07
N23-1white	10.87	6.11	1.52	1.83	15.73	0.16	61.46	0.03	0.04	0.23	1.71	0.02
N23-1red	1.02	7.12	1.255	2.72	22.89	0.31	54.14	0.04	0.07	0.26	9.71	0.01
N24-1grey	1.96	9.57	10.88	62.93	7.09	1.53	1.87	0.41	0.06	0.48	3.11	0.02
N25-1white	0.93	3.58	2.64	6.63	14.60	0.39	58.68	0.10	0.07	0.23	11.66	0.03
N25-1red	–	8.98	0.095	17.73	24.66	0.09	3.93	0.09	0.13	0.44	43.50	0.04
N26-1grey	3.75	17.35	6.37	49.53	3.42	0.62	14.80	0.31	0.08	0.15	3.24	0.09
N26-1white	4.84	11.89	5.06	33.82	6.43	0.62	34.06	0.28	0.08	0.46	2.05	0.06
N27-1grey	3.37	9.30	11.39	62.13	1.96	2.23	6.67	0.30	0.06	0.05	2.40	0.03

Table 2 The chemical composition of N23 and N25 before and after treatment

Samples	Wt%										
	Na_2O	MgO	Al_2O_3	SiO_2	SO_3	K_2O	CaO	TiO_2	Cr_2O_3	MnO	Fe_2O_3	CuO
N23 before	1.02	7.12	1.25	2.72	22.89	0.31	54.14	0.04	0.07	0.26	9.71	0.01
N23 after	1.38	2.04	8.76	37.45	16.17	1.05	1.37	0.51	0.02	0.16	30.95	0.01
N25 before	–	8.98	0.09	17.73	24.66	0.09	3.93	0.09	0.13	0.44	43.50	0.04
N25 after	4.46	6.53	2.30	10.30	16.08	0.30	7.68	0.12	0.10	0.39	51.32	0.04

boiling treatments, which illustrates the reduction of FeS_2. Besides, the characteristic diffraction peaks of Gypsum ($CaSO_4 \cdot 2H_2O$) almost vanish after the treatment (Fig. 5c),which implies the crystalline change or reduction of gypsum.

Physical heating exploration

Based on the microscopy, XRF and XRD results, a physical heating and boiling method was chosen. The white shellfish concretions began to loosen after heating method in the blast drying chamber. It could then, easily be pried up from the ceramic through the junction between shells and ceramics. Finally white shellfish concretion could be removed, as shown in Fig. 21(b). The same phenomenon happened with the gray concretions. The concretions became granular, fragile and could be straightforwardly removed by hands. This kind of concretions was also easily removed. As shown in Fig. 22(b), three different sizes of ceramics pieces appear after the treatment. For brown concretions (Fig. 23(a), Fig. 24(a)),

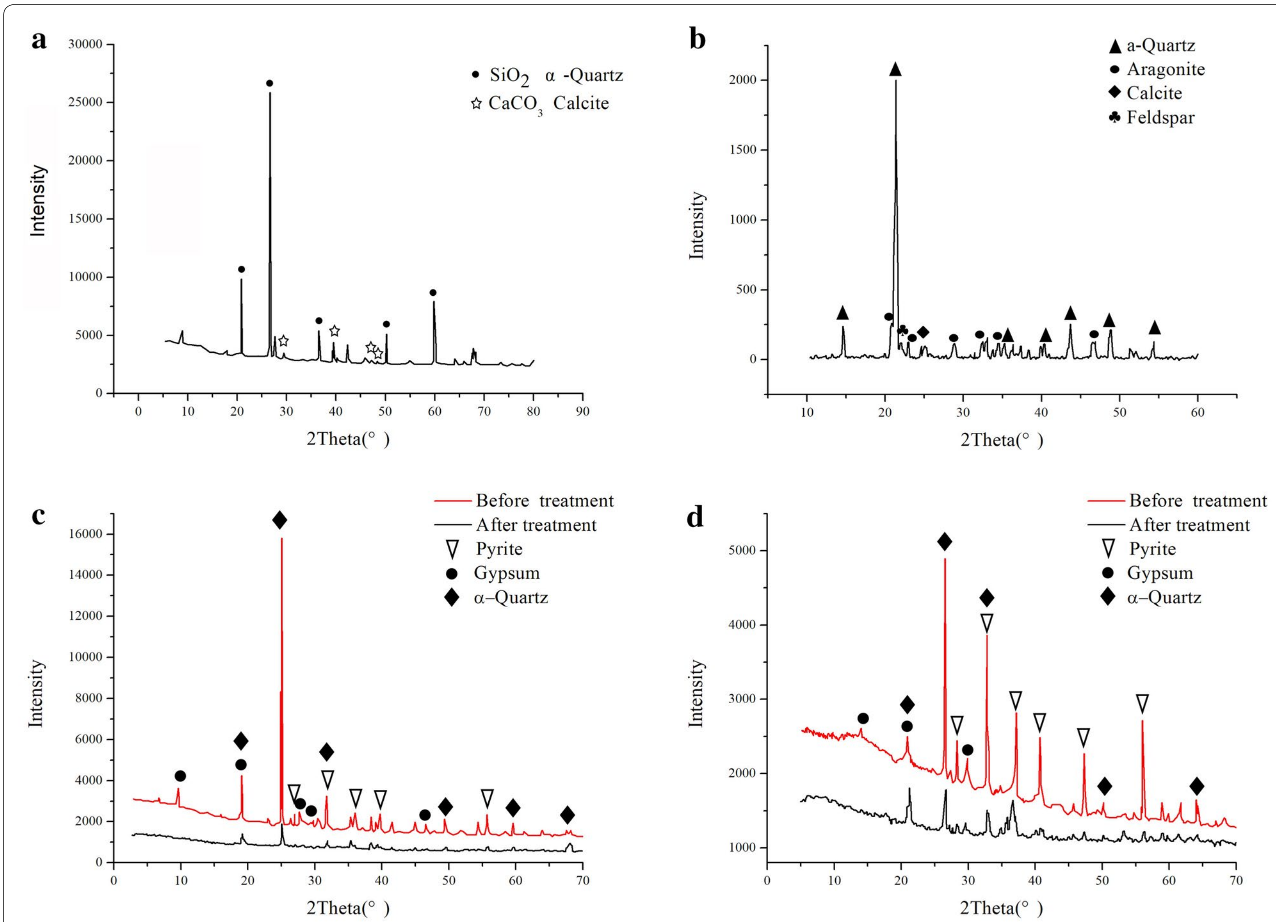

Fig. 5 **a** XRD spectrum of N26 sample; **b** XRD spectrum of sample N21; **c** comparative XRD spectrum of sample N23 before and after the treatment; **d** comparative XRD spectrum of sample N25 before and after the treatment

which contained red, dark red and brown particles, the interface was not that strong after 2–5 times of treatments of repeated heating and boiling. Although still hard, the concretions were possible to be removed by a scalpel. As shown in Fig. 23(b) and Fig. 24(b), serval smaller ceramics pieces present after removing the concretions. On the contrary, the shallow gray (Fig. 25) was very compact and hard after several attempts, so the method of heating and boiling didn't work here.

Compressive strength test

Table 3 sums up the results of compressive strength tests. Figure 6a and b are box diagrams of pottery and porcelain samples before and after repeated treatments. The compressive strength of both the pottery and porcelain were almost similar before and after physical heating. After the treatment, the compression range of the ceramics scarcely changed, which suggests that the heating and boiling process could do little harm to the ceramics.

Discussion

For the white shellfish concretions, microscopy observations show areas with what seems to be residues of mucus from the shells. Previous studies indicate that shellfish organisms like mussels could secrete a kind of adhesion protein with the name of Dopa in its foot protein, which usually helps shellfish organisms compactly attach to the surface of metals and rocks [16]. Generally, the higher proportion of Dopa the mussel contains, the more adhesive it would be [17]. So the reason why the shellfish concretions can easily be removed is probably related to the reduction of Dopa during the heating process.

Brown concretions are more complex because pyrite and gypsum coexist. According to the archaeological excavation [1], the "Nanhai I" shipwreck not only

Table 3 The compressive strength of samples

Pottery samples				Porcelain samples			
Before treatment		After treatment		Before treatment		After treatment	
Compressive strength (MPa)	Area of section (mm^2)	Compressive strength (MPa)	Area of section (mm^2)	Compressive strength (MPa)	Area of section (mm^2)	Compressive strength (MPa)	Area of section (mm^2)
13.20	133.67	13.20	127.74	137.20	176.64	112.50	161.17
17.00	115.09	14.40	127.87	146.90	168.92	133.50	179.98
12.60	149.26	12.30	122.77	105.80	174.85	106.00	177.13
17.10	157.89	18.30	135.56	143.20	179.66	98.90	199.61
13.30	124.28	16.10	110.50	92.20	171.86	100.90	177.77
12.50	141.73	12.50	118.52	94.80	175.24	141.80	171.77
12.70	140.70	19.10	117.68	102.80	179.17	138.00	170.72
18.70	111.53	13.80	125.10	117.60	164.14	121.40	158.41
15.50	123.71	16.90	129.94				

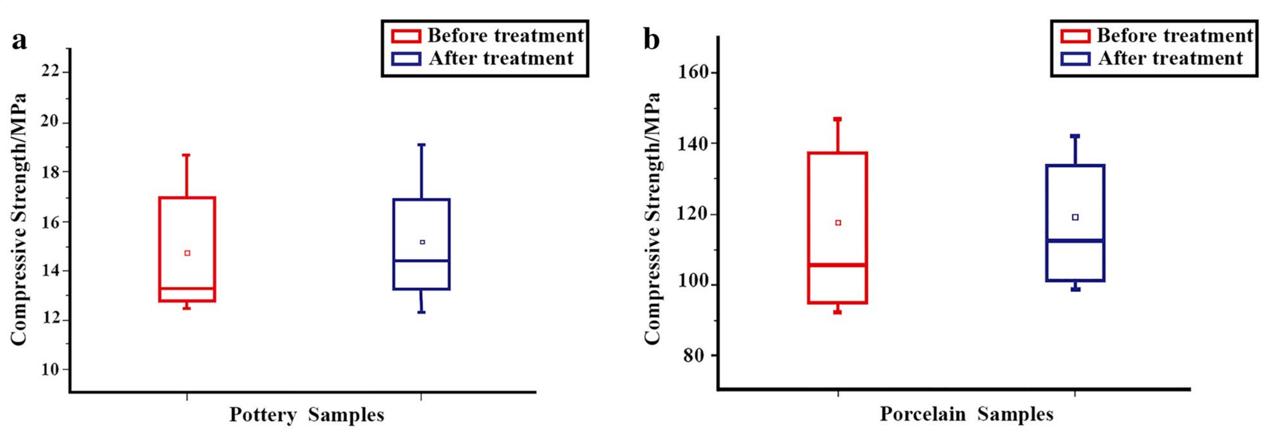

Fig. 6 Compressive strength comparison before and after treatment: **a** pottery samples; **b** porcelain samples

contained ceramics, but also had lots of iron products. Commonly, the formation of pyrite in sedimentary environments is closely associated with sulphate activity reducing bacteria; and if the supply of iron is sufficient, pyrite can easily form [18]. Meanwhile, the acidic condition in the seawater accelerates the dissolving of the biogenic shell and releasing of Ca^{2+}. Once the Ca^{2+} and SO_4^{2-} become over saturated, then gypsum is formed [19]. Based on the research above, it is not very difficult to deduce the origin of pyrite and gypsum in the brown concretions. Our experiments prove that this physical treatment is efficient on the white shellfish, gray and brown concretions. The chemical research indicates that Pyrite (FeS_2) can spontaneously be oxidized when exposed [20].

The chemical reaction is as follows:

$$4FeS_2 + 11O_2 \rightarrow 2Fe_2O_3 + 8SO_2 \uparrow + 3312.4KJ/mol.$$

In other words, when the samples with FeS_2 inside are exposed, a very slow oxidization happens, and they release a bit of SO_2. The released gases would expand the pores in the concretions. The pore-expansion is one of the factors responsible for the easy-removal of the concretions. On the other hand, the different expansions of both the ceramics and the concretions during the treatment are also an important factor causing the loosening of the brown concretions. In addition, Gypsum ($CaSO_4{\cdot}2H_2O$) is resolved in hot water ($CaSO_4{\cdot}2H_2O \leftrightharpoons Ca^{2+} + SO_4^{2-} + 2H_2O$) [21], and the repeated heating and boiling process reduce the Gypsum in the concretions, which more or less makes the concretions loosen.

Most gray concretions have porous textures according to micro-analyses. A long period of observation indicates that the surface particles of the gray concretions began to fall down in the indoor environment in Guangzhou, China. This means that temperature and humidity did have some effects. So the heating process could accelerate the evaporation of its interior gases such as H_2O, CO_2 and eventually make it loosen. In contrast, another group of concretions with a shallow gray appearance was still very hard and compact after several times of repeated heating and boiling. These concretions are a mix of lots of smaller sized sand grains and shell pieces with different shapes (Fig. 2), densely gathered together like cement blocks. Empirically, calcium carbonate found in concretion was regarded as fragments of shells since a substantial part of mollusk shells are composed of biologically formed calcite and aragonite [22]. However other smaller sized white grains are likely to be the result of chemical reactions in the sea; this will be studied in the future. Besides, the removal methods of the shadow gray concretions need more investigations.

Conclusions

Twenty-seven samples selected from the "Nanhai I" shipwreck were analyzed. The physical method of heating and boiling with few harm to the ceramic materials turns out to have some positive effects on the separation of white shellfish concretions, gray concretions and brown concretions. However, it cannot be used to remove the shadow gray concretions and a better removing method still needs to be found in the future.

Authors' contributions

XT, DY, HC provided the samples to be investigated in this study; YW and TZ carried out XRF, XRD, physical treatment analyses, and conducted a microscopy examination of the samples; GY provided his technical assistance during the comparing-treatment with modern materials; All authors read and approved the final manuscript.

Author details

[1] School of Sociology and Anthropology of Sun Yat-sen University, No.135, Xingangxi Rd, Guangzhou 510275, China. [2] Materials Science Institute, Sun Yat-sen University, Guangzhou 510275, China. [3] Maritime Silk Road Museum of Guangdong, Yangjiang 529535, China.

Acknowledgements

This research was financially supported by National Natural Foundation of China (Grant No. 41103013), Science and Technology Commission of Guang-Dong Province Project (2015B030803041) and the China Scholarship Council.

The authors would like to express gratitude to Mr. Xiaolong Feng (Sun-Yat-sen University, Guangzhou, China) for his technical assistance during XRD experiments.

Competing interests

The authors declare that they have no competing interests.

Ethics approval and consent to participate

Not applicable.

Publisher's Note

Received: 14 September 2017 Accepted: 7 January 2018
Published online: 01 February 2018

References

1. Zhang L. Cosmic voyage of "Nanhai I"shipwreck-An interview with Wei Jun, the director of underwater archaeological research center of Guangdong Cultural Relics and Archeology Institute, and Zhang Wei, captain of underwater archaeological team. China Award Sci Technol. 2007;12:22.
2. Ma Y, Hu D. Cobalt blue pigments on Ming Dynasty Jingdezhen blue-and-white-pircelain recovered from Nan'ao I shipwreck. J Natl Mus China. 2016;5:143–51.
3. Colomban P, Liem NQ, Sagon G, Tinh HX, Hoành TB. Microstructure, composition and processing of 15th century Vietnamese porcelains and celadons. J Cult Herit. 2003;4:187–97.
4. Rees-Jones S. Some aspects of conservation of iron objects from the sea. Stud Conserv. 1972;17:39–43.
5. Oddy W. A review of procedures for the conservation of cast and wrought iron found on the sea-bed. Int J Naut Archaeol. 1975;4:367–70.
6. North NA. Formation of coral concretions on marine iron. Int J Naut Archaeol. 1976;5:253–8.
7. North NA, Pearson C. Washing methods for chloride removal from marine iron artifacts. Stud Conserv. 1978;23:174–86.

8. MacLeod ID. Identification of corrosion products on non-ferrous metal artifacts recovered from shipwrecks. Stud Conserv. 1991;36:222–34.
9. Yang H, Tian X, Li N, Li X, Ma Q. Corrosion analysis of the copper artifacts salvaged from Ming Dynasty wreck ship at Nan'ao County, Guangdon, China. China Cult Herit Sci Res. 2012;3:87–91.
10. Yang H, Tian X, Li X, Ma Q. Analysis and removal of the concretion on the surface of the copper artifacts from Ming Dynasty wreck ship at Nan'ao county, Guangdong, China. China Cult Herit Sci Res. 2012;2:81–6.
11. Liu W, Zhang Z, Li X, Ma Q. Scientific analysis of concretions on the ancient marine iron recovered from three shipwrecks in the South China Sea. J Natl Mus China. 2011;2:145–56.
12. Ma Y. Research on desalination and protection of special undersea ceramics in Xisha. Collected papers of Chinese Chemical Society Conference. Guangzhou: Lingnan fine arts publishing house; 2004. p. 9–17.
13. Ma Y. Desalination and protection for the ceramics underwater in China. Mus Res. 2007;1:85–8.
14. Bao C. Corrosion and protection of marine-recovered iron artifacts from HuaGuang Reef I wreck. Corros Prot. 2012;7:614–25.
15. Standard test method for compressive resistance of ceramic materials (GB/T 4740-1999). Standardization administration of the People's Republic of China. Beijing. 1999. http://www.sac.gov.cn. Accessed 1 Feb 2000.
16. Han X. Single-molecule force spectroscopy study on Dopa adhesion. Master Dissertation. Nanjing: NanJing University of China; 2013. p. 1.
17. Akemi Ooka A, Garrell RL. Surface-enhanced Raman spectroscopy of DOPA-containing peptides related to adhesive protein of marine mussel, *Mytilus edulis*. Biopolymers. 2000;57:92–102.
18. Mozer A. Authigenic pyrite framboids in sedimentary facies of the Mount Wawel Formation (Eocene), King George Island, West Antarctica. Pol Polar Res. 2010;31:255–72.
19. Chen Z, Yan W, Chen M, Lu J, Gu S. Formation of authigenic gypsum and pyrite assemblage and its significance to gas ventings in Nansha Trough, South China Sea. Mar Geol Quat Geol. 2007;27:91–100.
20. Zhang H, Zhang C. Principle of pyrite spontaneous combustion and its prevention. Copper Eng. 2004;3:53–4.
21. Liu G, Ma L, Liu J. Physical property handbook of chemistry and chemical engineering: Inorganic volume. Beijing: Chemical Industry Press; 2002. p. 422.
22. Sun W, Jayaraman S, Chen W, Persson KA, Ceder G. Nucleation of metastable aragonite $CaCO_3$ in seawater. Proc Natl Acad Sci. 2015;112:3199–204.